

correspond to structures **1a** and **2a**, respectively.

Neutral product studies show that free fluoroethyl ions convert to the most stable structure (**2a**), as had previously been shown by collisional activation mass spectrometry.⁶ In these ions, hydrogen and fluorine shifts occur one after the other. Regardless of the order in which these sequential transpositions occur, free ions that are formed and neutralized on the millisecond time scale isomerize to α -fluoroethyl cations before they can be interrogated. On the other hand, over much shorter intervals, decompositions of ion-neutral complexes, which occur on the subnanosecond time scale, afford a glimpse of the antecedent rearrangements. The

implications of this are the subject of continuing investigations.

Acknowledgment. This work was supported by NSF Grants CHE 8802086 and CHE 9203066. We are grateful to Dr. Thomas Shaler and Dr. Dan Borchardt for experimental assistance and useful discussions.

Supplementary Material Available: A figure showing observed and simulated ¹H NMR spectra for **8a**, tabulated solutions for Schemes I and II, and tables of SCF-calculated geometries and normal modes for the structures in Figure 1 (16 pages). Ordering information is given on any current masthead page.

Characterization of Iron-Sulfur Cubane Clusters by Fast Atom Bombardment Mass Spectrometry: The Formation of Ionic $[\text{Fe}_m\text{S}_n]$ Clusters through Gas-Phase Unimolecular Reduction Processes and Their Solution Parallels

Wen-Lian Lee,^{1a} Douglas A. Gage,^{1b} Zhi-Heng Huang,^{1b} Chi K. Chang,^{*,1a} Mercuri G. Kanatzidis,^{*,1a} and John Allison^{*,1a}

Contribution from the Departments of Chemistry and Biochemistry, Michigan State University, East Lansing, Michigan 48824. Received October 15, 1991

Abstract: Fast atom bombardment mass spectrometry (FAB-MS) has been used to analyze a series of iron-sulfur clusters $(\text{A})_2\text{Fe}_4\text{S}_4\text{X}_4$, where $\text{A} = \text{R}_4\text{N}$ or Ph_4P and $\text{X} = \text{Cl}, \text{Br}, \text{SET}, \text{SPh}$. A cluster with mixed Cl, SPh ligands was also studied. The usefulness of the FAB technique in characterizing these and related biologically-relevant complexes is evaluated. The best FAB-MS results for these clusters were obtained with 3-nitrobenzyl alcohol (NBA) and 2-nitrophenyl octyl ether (NPOE) as matrices. The most unique feature of the negative ion FAB mass spectra is the identification of the intact iron core $[\text{Fe}_4\text{S}_4\text{X}_4]^-$, preformed anions $[(\text{A})\text{Fe}_4\text{S}_4\text{X}_4]^-$, and a series of cluster fragment ions. A mechanism is proposed to explain the formation of small $[\text{Fe}_m\text{S}_n]$ clusters through unimolecular reduction processes that involve only +2 and +3 oxidation states for the Fe atoms. This work demonstrates that FAB-MS can be employed as a valid method for rapid molecular weight determination as well as structural elucidation of $[\text{Fe}_4\text{S}_4]$ cluster-containing complexes.

Introduction

Proteins containing iron-sulfur clusters frequently serve as redox enzymes and participate in electron-transfer reactions associated with processes such as photosynthesis, nitrite reduction, and nitrogen fixation.^{2,3} At present, four distinct types of Fe-S cluster cores, in various oxidation states, have been identified in such enzymes: FeS_4 , Fe_2S_2 , Fe_3S_4 , and Fe_4S_4 . The iron centers in these clusters form bridges in proteins, usually by bonding to sulfur atoms of cysteine residues. Most of these clusters participate in one-electron redox processes.⁴ They frequently contain iron atoms in one or more oxidation states, usually Fe^{3+} and Fe^{2+} . A variety of iron/sulfur core oxidation states have been established for the various Fe/S clusters present in proteins. Those identified to date include the following: $[\text{Fe}_2\text{S}_2]^{1+,2+}$, $[\text{Fe}_3\text{S}_4]^{0,1+}$, and $[\text{Fe}_4\text{S}_4]^{1+,2+,3+}$.

In view of the diversity of structures and biological functions, these complexes are difficult to characterize by direct studies of the proteins themselves. Fortunately, synthetic analogs of the mono-, bi-, and tetrairon centers have been developed to provide insights into their intrinsic properties in the absence of protein-imposed constraints. Of the structurally characterized synthetic

models for the various $[\text{Fe}_m\text{S}_n]$ clusters now available, the cubane-type, $[\text{Fe}_4\text{S}_4]$, core geometry appears to be the most commonly encountered, and it has been the focus of an intensive body of structural, spectroscopic, and magnetic studies for the last two decades.^{5,6} A wide variety of model complexes of the type $[\text{Fe}_4\text{S}_4\text{X}_4]^{2-}$ have been made in which the anionic components, X^- , are a variety of thiolates (SR^-),⁶ halides (Cl^- , Br^- , and I^-),^{7,8} and alkoxides (OR^-),⁹ as well as combinations of these ligands.¹⁰

(5) (a) Holm, R. H. *Acc. Chem. Res.* 1977, 10, 427. (b) Berg, J. M.; Holm, R. H. In *Iron-Sulfur Proteins*; Spiro, T. G., Ed.; Wiley-Interscience: New York, 1982; p 1.

(6) Averill, B. A. In *Metal Clusters in Proteins*. Que, L., Jr., Ed. *ACS Symp. Ser.* 1988, No. 372, 258.

(7) (a) Hagen, K. S.; Reynolds, J. G.; Holm, R. H. *J. Am. Chem. Soc.* 1981, 103, 4054. (b) Hagen, K. S.; Holm, R. H. *J. Am. Chem. Soc.* 1982, 104, 5496. (c) Hagen, K. S.; Watson, A. D.; Holm, R. H. *J. Am. Chem. Soc.* 1983, 105, 3905. (d) Wong, G. B.; Bobrik, M. A.; Holm, R. H. *Inorg. Chem.* 1978, 17, 578. (e) Johnson, R. W.; Holm, R. H. *J. Am. Chem. Soc.* 1978, 100, 5338.

(8) (a) Coucouvanis, D.; Kanatzidis, M.; Simhon, E.; Baenziger, D. C. *J. Am. Chem. Soc.* 1982, 104, 1874. (b) Kanatzidis, M. G.; Salifoglou, A.; Coucouvanis, D. *Inorg. Chem.* 1986, 25, 2460.

(9) Cleland, W. E., Jr.; Holtman, D. A.; Sabat, M.; Ibers, J. A.; Defotis, G. C.; Averill, B. A. *J. Am. Chem. Soc.* 1983, 105, 6021. (b) Cleland, W. E., Jr.; Averill, B. A. *Inorg. Chim. Acta* 1985, 106, L17.

(10) (a) Kanatzidis, M. G.; Ryan, M.; Coucouvanis, D.; Simopoulos, A.; Kostikas, A. *Inorg. Chem.* 1983, 22, 179. (b) Johnson, R. E.; Papaefthymiou, G. C.; Frankel, R. B.; Holm, R. H. *J. Am. Chem. Soc.* 1983, 105, 7280. (c) Kanatzidis, M. G.; Baenziger, N. C.; Coucouvanis, D.; Simopoulos, A.; Kostikas, A. *J. Am. Chem. Soc.* 1984, 106, 4500. (d) Kanatzidis, M. G.; Coucouvanis, D.; Simopoulos, A.; Kostikas, A.; Papaefthymiou, V. *J. Am. Chem. Soc.* 1985, 107, 4925.

(1) (a) Department of Chemistry. (b) Department of Biochemistry.
 (2) Thauer, R. K.; Schoenheit, P. In *Iron-Sulfur Proteins*; Spiro, T. G., Ed.; Wiley Interscience: New York, 1982; p 329.
 (3) Thompson, A. J. In *Metalloproteins*; Harrison, P., Ed.; Verlag Chemie: Weinheim, FRG, 1985; Part 1, p 79.
 (4) (a) Carter, C. W.; Kraut, J.; Freer, S. T.; Alden, R. A.; Sieker, L. C.; Adman, E.; Jensen, L. H. *Proc. Natl. Acad. Sci. U.S.A.* 1972, 68, 3526. (b) Herskovitz, T.; Averill, B. A.; Holm, R. H.; Ibers, J. A.; Phillips, W. D.; Weiher, J. F. *Proc. Natl. Acad. Sci. U.S.A.* 1972, 69, 2437.

Recently, the "subsite-differentiated" analogs of biological $[\text{Fe}_4\text{S}_4]^{2+}$ clusters,^{11,12} as well as synthetic peptide model complexes,¹³⁻¹⁵ have also been explored. Generally, the characterization of such compounds has always relied on UV-visible spectroscopy, elemental analysis, NMR spectroscopy (where applicable for complexes in solution), and single-crystal X-ray crystallography.

Although conventional electron impact mass spectrometry is a standard spectroscopic method for the characterization of inorganic compounds, it is not readily applicable for the analysis of ionic, nonvolatile compounds such as those that contain the $[\text{Fe}_4\text{S}_4\text{X}_4]^{2-}$ core. Recently, fast atom bombardment (FAB) ionization¹⁶ has been used for the mass spectrometric analysis of a variety of inorganic compounds including classical inorganic salts, organometallic compounds, coordination complexes, and bioinorganic systems.¹⁷ The main advantage of FAB-MS¹⁸ and the related techniques of liquid secondary ion mass spectrometry (LSIMS)¹⁹ is the facility with which ions can be generated from nonvolatile/thermally labile inorganic compounds. Successful completion of the experiment frequently depends on an appropriate choice of the viscous liquid matrix to assist in the desorption and ionization processes.

This is the first report documenting the utility of FAB-MS for the characterization of $[\text{Fe}_4\text{S}_4\text{X}_4]^{2-}$ clusters. Results of both positive and negative ion FAB-MS are presented here in the characterization of a series of salts of anionic iron-sulfur clusters which include the following: (a) $(\text{A})_2\text{Fe}_4\text{S}_4\text{Br}_4$, A = Bu_4N , Pr_4N , Et_4N ; (b) $(\text{A})_2\text{Fe}_4\text{S}_4\text{Cl}_4$, A = $(\text{Ph}_3\text{P}=\text{N})_2$ (PPN), Ph_4P , Bu_4N , Me_4N ; (c) $(\text{A})_2\text{Fe}_4\text{S}_4(\text{SPh})_4$, A = Ph_4P , Bu_4N ; (d) $(\text{A})_2\text{Fe}_4\text{S}_4(\text{SEt})_4$, A = Ph_4P , Ph_4As ; and (e) $(\text{Ph}_4\text{P})_2\text{Fe}_4\text{S}_4(\text{SPh})_2\text{Cl}_2$. The results reported herein demonstrate that useful mass spectra can be obtained by choosing proper matrices. When negative ion FAB is employed, identification of the intact core, as the univalent anion, $[\text{Fe}_4\text{S}_4\text{X}_4]^-$, is straightforward. Thus, FAB-MS analysis can be employed as a valid method for rapid molecular weight determination. A variety of fragment ions have also been observed; mechanisms for their formation are proposed.

The mass spectral results show that, in the gas phase, the iron-sulfur cubane core undergoes unimolecular dissociation following desorption/ionization. The fragment ions, which contain 4, 3, and 2 iron atoms, have interesting parallels with known species that have been synthesized/identified in condensed-phase studies. These parallels, and their implications, will be discussed.

Experimental Section

Mass spectrometric analyses were performed on a JEOL HX-110 HF double-focusing mass spectrometer, operated in either positive ion or negative ion mode. Ions were produced by fast atom bombardment (FAB) with a beam of 6-keV Xe atoms or by LSIMS using a 20-keV cesium ion beam. The mass spectrometer was operated with an accelerating voltage of 10 kV and a resolution of at least 3000. The instrument was scanned at a rate of 2 min over the range of 1-6000 Da. Data reported represent mass spectra obtained in a single scan.

A variety of liquid matrices including glycerol, thioglycerol, 3-nitrobenzyl alcohol (NBA), and 2-nitrophenyl octyl ether (NPOE) were

evaluated. Glycerol and thioglycerol both lead to significant complicated additions to the ionic clusters formed. The terminal ligand-matrix exchange reactions such as dehalogenation²⁰ or ligand substitution have been observed.²¹ Both NPOE and NBA were found to be most appropriate for analyzing complexes that contain halide ligands,²² because reactions between analytes and matrices do not occur. Iron-sulfur clusters with thiolate ligands also show sensitivity to the matrix NBA, and only NPOE was found to be a suitable matrix in those cases. Samples to be analyzed were dissolved in dimethyl formamide (DMF), and 1 μL of the solution (ca. 10 mM) was mixed with 2 μL of the matrix (NBA or NPOE) on the FAB probe tip.

The iron-sulfur cluster complexes were prepared and purified by published procedures.^{7,10} The purity of the complexes was generally established by UV-visible spectroscopy, ¹H-NMR spectroscopy, and X-ray powder pattern analysis. To avoid oxidation, all of the samples were handled under a flow of pure nitrogen during their preparation and introduction into the mass spectrometer.

Results and Discussion

1. Mass Spectral Characterization of Iron-Sulfur Clusters.

Presented here are experimental results and observations in the FAB-MS analysis of various salts containing the iron-sulfur cubane core. As will be shown, positive FAB-MS gives molecular weight and structural information for the analytes $(\text{A})_2\text{Fe}_4\text{S}_4\text{Br}_4$ and $(\text{A})_2\text{Fe}_4\text{S}_4\text{Cl}_4$. However, the positive ion FAB-MS studies of complexes containing thiolate ligands $(\text{A})_2\text{Fe}_4\text{S}_4(\text{SPh})_4$ and $(\text{A})_2\text{Fe}_4\text{S}_4(\text{SEt})_4$, as well as mixed ligand complex $(\text{Ph}_4\text{P})_2\text{Fe}_4\text{S}_4(\text{SPh})_2\text{Cl}_2$, gave limited information related to the molecular formula. In contrast, negative ion mass spectra of all iron-sulfur cubanes display peaks representing the unique features of the intact $[\text{Fe}_4\text{S}_4\text{X}_4]^-$ core, as well as a variety of fragment ions.

Since most of the ions observed contain atoms that have a number of isotopic forms, isotopic clusters of peaks are observed to represent a single elemental formula. In the following discussion, the nominal m/z value is used to represent an ion of a given composition, calculated by using the most abundant isotope of each element present (i.e., 56 u for Fe, 35 u for Cl, 79 u for Br, and 32 u for S). In the data presented, reported relative intensities represent the most abundant isotopic peak of an isotopic cluster of mass spectral peaks.

A. Positive and Negative Ion FAB Mass Spectra of Halogenated Clusters $(\text{A})_2\text{Fe}_4\text{S}_4\text{Br}_4$ and $(\text{A})_2\text{Fe}_4\text{S}_4\text{Cl}_4$. Both NBA and NPOE are suitable matrices for positive and negative ion FAB-MS studies of $(\text{A})_2\text{Fe}_4\text{S}_4\text{X}_4$ compounds, where X = Br, and Cl. In general, when FAB is used in the analysis of ionic analytes of the form $[\text{A}^+][\text{B}^-]$, the intact cation $[\text{A}]^+$, and possibly its fragment ions, will dominate the positive ion mass spectrum, while $[\text{B}^-]$ and charged fragments therefore will be present in the negative ion spectrum. In the FAB-MS analysis of these ionic complexes, which can be written as $(\text{A}^+)_2[\text{Fe}_4\text{S}_4]^{2+}(\text{X}^-)_4$, the cation (A^+) is seen as the base peak in the positive ion spectra. However, the positive ion FAB spectra are disappointing in that they give limited structural information in the mass range below m/z 800. Most of the peaks in this range are due to the ions formed from interactions between the intact cation, A^+ , and matrix molecules, to yield adduct ions of the type $[\text{NBA}_n + \text{A}]^+$ or molecular fragments that do not contain either iron or sulfur, such as $[2(\text{A}) + \text{X}]^+$. However, the most significant spectral features in the positive ion spectra are three clusters of peaks in the higher mass range. In the positive ion spectrum of $(\text{Et}_4\text{N})_2\text{Fe}_4\text{S}_4\text{Br}_4$ as shown in Figure 1, the significant high mass ions represent the ionic species $[(\text{Et}_4\text{N})_2\text{Fe}_4\text{S}_4\text{Br}_3]^+$ (m/z 849), $[(\text{Et}_4\text{N})_2\text{Fe}_4\text{S}_4\text{Br}_4]^+$ (m/z 928), and $[(\text{Et}_4\text{N})_3\text{Fe}_4\text{S}_4\text{Br}_4]^+$ (m/z 1058), respectively. These can also be written as variants of the neutral salt molecule, M, as $[\text{M} - \text{Br}]^+$, $[\text{M}]^+$, and $[\text{M} + \text{A}]^+$, respectively. The gas-phase $[\text{M} + \text{A}]^+$ adduct represents the peak at the highest m/z value in the spectrum and is presumably formed by complexation of the $(\text{Et}_4\text{N})^+$ cation with the desorbed neutral $(\text{Et}_4\text{N})_2\text{Fe}_4\text{S}_4\text{Br}_4$

(11) Holm, R. H.; Ciurli, S.; Weigel, J. A. *Prog. Inorg. Chem.* **1990**, *38*, 1.

(12) (a) Stack, T. D. P.; Weigel, J. A.; Holm, R. H. *Inorg. Chem.* **1990**, *29*, 3745. (b) Ciurli, S.; Carrie, M.; Weigel, J. A.; Carney, M. J.; Stack, T. D. P.; Papaefthymiou, G. C.; Holm, R. H. *J. Am. Chem. Soc.* **1990**, *112*, 2654. (c) Weigel, J. A.; Holm, R. H.; Srivastava, K. K. P.; Munck, E. *J. Am. Chem. Soc.* **1990**, *112*, 8015. (d) Whitener, M. A.; Peng, G.; Holm, R. H. *Inorg. Chem.* **1991**, *30*, 2411. (e) Weigel, J. A.; Holm, R. H. *J. Am. Chem. Soc.* **1991**, *113*, 4184.

(13) Nakamura, A.; Ueyama, N. In *Metal Clusters in Proteins*; Que, L., Jr., Ed.; ACS Symp. Ser. No. 372; American Chemical Society: Washington, DC, 1988; p 292.

(14) Nakamura, A.; Ueyama, N. *Adv. Inorg. Chem.* **1989**, *33*, 39.

(15) (a) Ohno, R.; Ueyama, N.; Nakamura, A. *Chem. Lett.* **1989**, 399. (b) Ohno, R.; Ueyama, N.; Nakamura, A. *Inorg. Chim. Acta* **1990**, 253.

(16) Barber, M.; Bordoli, R. S.; Sedgwick, R. D.; Tyler, A. N. *J. Chem. Soc., Chem. Commun.* **1981**, 325.

(17) Miller, J. M. *Mass Spectrom. Rev.* **1989**, *9*, 319 and references therein.

(18) Fenselau, C.; Cotter, R. J. *Chem. Rev.* **1987**, *87*, 501.

(19) Pachuta, S. J.; Cooks, R. G. *Chem. Rev.* **1987**, *87*, 647.

(20) Sethi, S. K.; Nelson, C. C.; McClosky, J. A. *Anal. Chem.* **1984**, *56*, 177.

(21) Divisia-Blohorn, B.; Kyriakov, G.; Ulrich, J. *Org. Mass Spectrom.* **1985**, *22*, 463.

(22) Hegetscheveler, K.; Keller, T.; Amrein, W.; Schneider, W. *Inorg. Chem.* **1991**, *30*, 873.

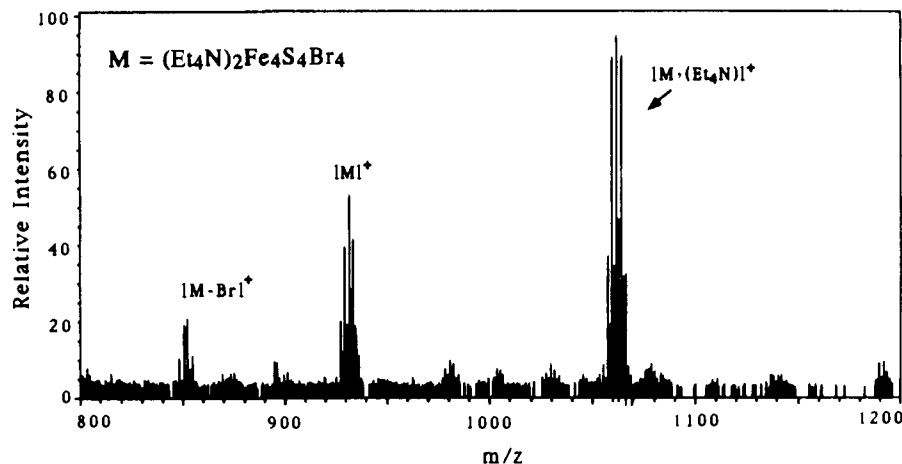


Figure 1. A portion of the positive ion FAB mass spectrum of $[(\text{Et}_4\text{N})_2\text{Fe}_4\text{S}_4\text{Br}_4]$ (M), using the matrix NBA.

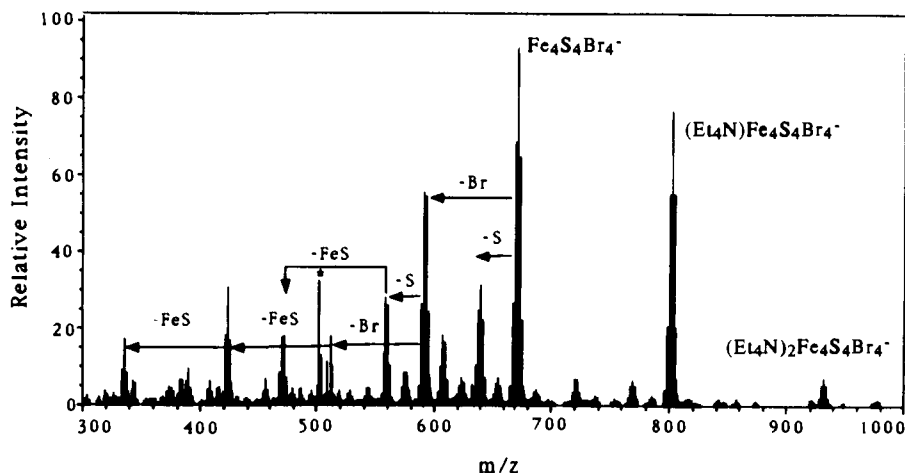


Figure 2. Negative ion FAB mass spectrum of $[(\text{Et}_4\text{N})_2\text{Fe}_4\text{S}_4\text{Br}_4]$ using the matrix NPOE. Matrix ions are designated with an asterisk.

molecule. The molecular ion peak, $[(\text{Et}_4\text{N})_2\text{Fe}_4\text{S}_4\text{Br}_4]^+$, which provides direct molecular weight information, is also observed. Thus, if a compound (M) of the type $(\text{A}^+)_2\text{Fe}_4\text{S}_4(\text{X}^-)_4$ is being characterized by FAB-MS in the positive ion mode, spectra similar to Figure 1 will be generated. There will be three sets of high mass peaks representing the chemical species $[\text{M} - \text{X}]^+$, $[\text{M}]^+$, and $[\text{M} + \text{A}]^+$. The middle set of peaks, representing $[\text{M}]^+$, will directly provide the molecular weight of the compound. The peaks at higher and lower m/z values, when compared to those representing $[\text{M}]^+$, provide primary information on the masses of X and A. At this point, an analysis of the isotopic distributions and/or exact mass measurements on any of these ionic species would lead to an unambiguous elemental formula.

In contrast, the negative ion FAB mass spectrum of $(\text{Et}_4\text{N})_2\text{Fe}_4\text{S}_4\text{Br}_4$ (Figure 2), obtained using the matrix NPOE, is much richer than the cation spectrum. Dominant high mass ions include the $[\text{M} - \text{A}]^-$ complex, formed by loss of a tetraethylammonium cation, at m/z 798. The intact iron-sulfur cubane, as a -1 ion, $[\text{Fe}_4\text{S}_4\text{Br}_4]^-$ (m/z 668) is also observed. The molecular anion $[(\text{Et}_4\text{N})_2\text{Fe}_4\text{S}_4\text{Br}_4]^-$ (m/z 928) is present in the negative ion spectrum, but the peak is of very low intensity. The positive and negative ion FAB mass spectra of halogenated complexes such as $(\text{A})_2\text{Fe}_4\text{S}_4\text{Br}_4$ and $(\text{A})_2\text{Fe}_4\text{S}_4\text{Cl}_4$ give similar spectra to that shown for $(\text{Et}_4\text{N})_2\text{Fe}_4\text{S}_4\text{Br}_4$, and these spectra are tabulated in Tables I and II. All of the elemental formulas listed for the ions observed were confirmed on the basis of the close agreement of observed/calculated isotopic distributions for the molecular formulas listed. Thus, the formula weight of the complex could be deduced from these clusters of mass spectral peaks without ambiguity. As an example, graphs a and b in Figure 3 show the comparison between calculated and observed isotopic abundances of $[(\text{Et}_4\text{N})_2\text{Fe}_4\text{S}_4\text{Br}_4]^+$ and $[\text{Fe}_4\text{S}_4\text{Br}_4]^-$, respectively. By com-

Table I. Cations in the FAB Mass Spectra of Complexes $(\text{A})_2\text{Fe}_4\text{S}_4\text{X}_4$ (Designated as M), X = Br and Cl, Using the Matrix NBA^a

	$(\text{A})_2\text{Fe}_4\text{S}_4\text{Br}_4$ for A =			$(\text{A})_2\text{Fe}_4\text{S}_4\text{Cl}_4$ for A =			
	Et_4N	Pr_4N	Bu_4N	Me_4N	Bu_4N	Ph_4P	PPN^b
$[\text{M} + \text{A}]^+$	1058 (100)	1226 (100)	1394 (100)	714 (100)	1218 (100)	1509 (100)	2106 (100)
$[\text{M}]^+$	928 (52)	1040 (45)	1152 (10)	640 (32)	976 (32)	1170 (16)	1568 (41)
$[\text{M} - \text{X}]^+$	849 (23)	961 (35)	1117 (11)	605 (19)	931 (9)	1135 (12)	1533 (10)

^aNumbers in the table refer to the nominal m/z value and the relative intensities of the identified ions. Intensities, listed in parentheses, are relative to 100 for the most abundant analyte ion listed. ^bPPN = $(\text{Ph}_3\text{P})_2\text{N}^+$. ^c $[\text{M} + \text{A}]^+ = [(\text{A})_3\text{Fe}_4\text{S}_4\text{X}_4]^+$, $[\text{M}]^+ = [(\text{A})_2\text{Fe}_4\text{S}_4\text{X}_3]^+$, and $[\text{M} - \text{X}]^+ = [(\text{A})_2\text{Fe}_4\text{S}_4\text{X}_2]^+$.

paring the spectra from both positive and negative ion FAB-MS studies, a rapid molecular weight determination of iron-sulfur cubane complexes has been successfully achieved.

In addition to peaks that provide molecular weight information, Figure 2 exhibits several other peaks formed by fragmentation of the iron-sulfur cubane core. Fragment ions represented by the quartet at m/z 589, 591, 593, 595 and the triplet at m/z 510, 512, 514 correspond to anionic species $[\text{Fe}_4\text{S}_4\text{Br}_3]^-$ and $[\text{Fe}_4\text{S}_4\text{Br}_2]^-$, respectively. The relatively low intensity quartet at m/z 719, 721, 723, 725 corresponds to the formula $[(\text{Et}_4\text{N})\text{Fe}_4\text{S}_4\text{Br}_3]^-$. Surprisingly, we observed a number of abundant anionic fragments of the $[\text{Fe}_4\text{S}_4\text{Br}_4]$ core structure. For example, the fragment $[\text{Fe}_4\text{S}_3\text{Br}_4]^-$ appears at m/z 636–644, $[\text{Fe}_4\text{S}_3\text{Br}_3]^-$ is formed and is seen at m/z 557–563, $[\text{Fe}_3\text{S}_2\text{Br}_3]^-$ is present at m/z 469–475, $[\text{Fe}_3\text{S}_3\text{Br}_2]^-$ is seen at m/z 422–426, and $[\text{Fe}_2\text{S}_2\text{Br}_2]^-$ is seen at m/z 334–338. In each of these groups of peaks, the bromine content dominates the isotopic "fingerprint" pattern, which allows

Table II. Relative Intensities of Anions in the Negative Ion FAB Mass Spectra of Complexes (A)₂Fe₄S₄X₄, X = Br and Cl, Using the Matrix NPOE

ions observed	relative intensities ^a						
	(A) ₂ Fe ₄ S ₄ Br ₄ for A =			(A) ₂ Fe ₄ S ₄ Cl ₄ for A =			
	Et ₄ N	Pr ₄ N	Bu ₄ N	Me ₄ N	Bu ₄ N	Ph ₄ P	(Ph ₃ P=) ₂ N
[(A) ₂ Fe ₄ S ₄ X ₄] ⁻	11	7					
[(A)Fe ₄ S ₄ X ₄] ⁻	82	78	25	55	52	53	42
[(A)Fe ₄ S ₄ X ₃] ⁻	11	11	14				
[Fe ₄ S ₄ X ₄] ⁻	100	100	100	100	100	100	100
[Fe ₄ S ₃ X ₄] ⁻	33	39	42	40	32	28	32
[Fe ₄ S ₄ X ₃] ⁻	60	78	87	78	70	47	60
[Fe ₄ S ₃ X ₃] ⁻	30	37	55	45	5	12	15
[Fe ₄ S ₄ X ₂] ⁻	19	26	43	35	37	18	27
[Fe ₄ S ₃ X ₂] ⁻				9	9	8	7
[Fe ₄ S ₄ X ₁] ⁻				10	15	12	9
[Fe ₃ S ₃ X ₃] ⁻	20	30	39	45	65	8	28
[Fe ₃ S ₃ X ₂] ⁻	33	53	60	65	90	15	39
[Fe ₂ S ₂ X ₂] ⁻	18	55	12	40	55	47	33

^a Intensities are relative to 100 for the most abundant analyte ions.

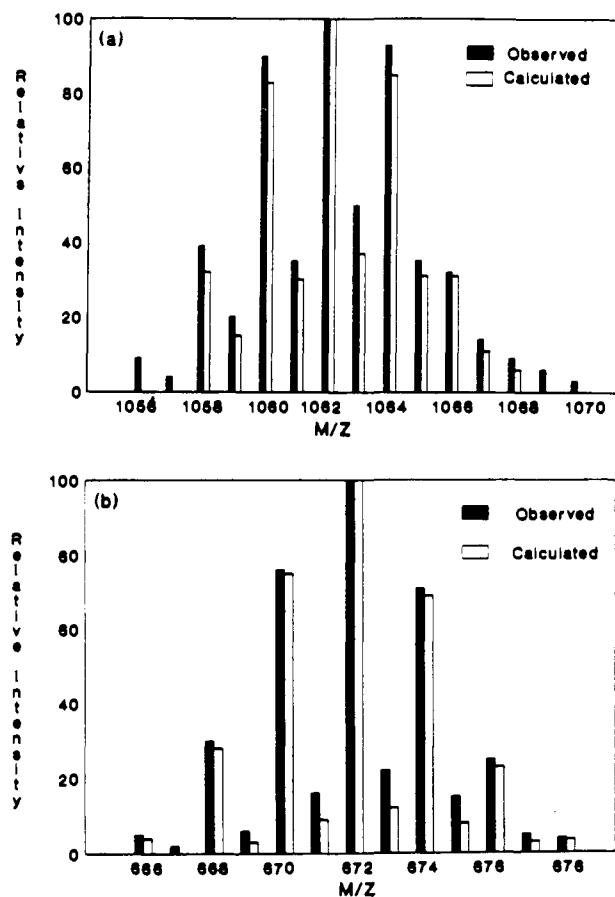


Figure 3. Comparison of isotope abundance for an experimentally observed (solid bar) and theoretically calculated (open bar) cluster: (a) [(Et₄N)₃Fe₄S₄Br₄]⁺ and (b) [Fe₄S₄Br₄]⁻.

a facile identification of these various fragment ions. The rich fragmentation observed in negative ion FAB-MS is also important in establishing the presence of the intact [Fe₄S₄] cubane core. Additional features of the negative ion spectrum that should be noted are the low-intensity signals appearing 16 u and/or 32 u above each of the major fragment peaks. These are most likely due to oxygen atom transfer reactions involving matrix molecules such as NBA or NPOE. Oxygen additions have been observed before in the FAB-MS of organometallic compounds.²³ The chemistry may well take place in the gas phase, between iron-

sulfur-containing anions and individual matrix molecules. In support of this possibility, we note that McElvany and Allison²⁴ have reported the gas-phase, bimolecular chemistry of transition-metal-containing anions such as Fe(CO)₃⁻ with *n*-nitroalkanes, using ion cyclotron resonance (ICR) mass spectrometry. In these systems, products such as [Fe(CO)₃O]⁻ are formed due to oxo transfer from the NO₂ group of the organic molecule. Oxygen incorporation is also possible via S/O exchange processes. This has recently been observed in laser vaporization studies of a metal sulfide, Al₂S₃.²⁵ Such a reaction is reasonable for aluminum compounds, since the Al-O bond is approximately 20 kcal/mol stronger than the Al-S bond. However, the situation is reversed for Fe, with the bond to S being much stronger than that to O. Thus, it is unlikely that oxygen incorporation occurs by an S/O exchange reaction.

The negative ion FAB mass spectra of these iron-sulfur cubanes are dominated by ions with a net charge of -1. Of particular interest in these experiments would be the detection of the doubly-charged core [Fe₄S₄Br₄]²⁻. This ion has the same nominal mass as the singly-charged fragment [Fe₂S₂Br₂]⁻. The two species can be easily distinguished, since the -1 ion will exhibit isotopic peaks due to the presence of Br, which will be separated by 2 *m/z* units. If the doubly-charged anion peak is present, it will have the same nominal mass, but a much richer isotopic pattern, since it contains four bromine atoms. In addition, for the -2 ion, the major isotopic peaks will be separated by 1 *m/z* unit. Doubly-charged ions have been previously reported in the FAB analysis of transition-metal-containing compounds. For example, abundant doubly-charged cations, such as [Ru(bpy)₃]²⁺, from ruthenium(II) complexes, have been generated in FAB mass spectrometry.²⁶ The spectrum of (Et₄N)₂Fe₄S₄Br₄ (Figure 2) reveals an isotopic cluster of peaks with a nominal *m/z* value of 334; however, careful analysis of the isotopic pattern indicates that no peaks due to [Fe₄S₄Br₄]²⁻ are present; the *m/z* 334-containing cluster of peaks only represents the anion [Fe₂S₂Br₂]⁻. In this case, the doubly-charged anion may not be a stable species in the gas phase. While the dianion certainly exists in solution, there are a number of reasons why it may not be observed in the FAB experiment. In the desorption process, it may transfer an electron to the nitroaromatic matrix, following a lower energy pathway. Even if the dianion is desorbed intact, it may either eject an electron spontaneously or lose an electron in a subsequent collision with a desorbed matrix molecule.

B. Negative Ion FAB Mass Spectra of Thiolated Iron-Sulfur Cubane Clusters (A)₂Fe₄(SR)₄, R = Ph and Et. Our experience with the halide-containing Fe/S compounds demonstrated that

(24) McElvany, S. W.; Allison, J. *Organometallics* 1986, 5, 1219.

(25) Parent, D. C. *Chem. Phys. Lett.* 1991, 183, 45.

(26) (a) Bojesen, G. *Org. Mass Spectrom.* 1985, 20, 415. (b) Miller, J. M.; Balasumugan, K.; Nye, J.; Deacon, G. B.; Thomas, N. C. *Inorg. Chem.* 1987, 26, 560. (c) Liang, X.; Suwanrumpha, S.; Freas, R. B. *Inorg. Chem.* 1991, 30, 652.

(23) (a) Kowalski, M. H.; Sharp, T. R.; Stang, P. J. *Org. Mass Spectrom.* 1987, 22, 642. (b) Boyle, P. D.; Johnson, B. J.; Alexander, B. D.; Casalnuovo, J. A.; Gannon, P. R.; Johnson, S. M.; Larka, E. A.; Muetting, A. M.; Pignolet, L. H. *Inorg. Chem.* 1987, 26, 1346.

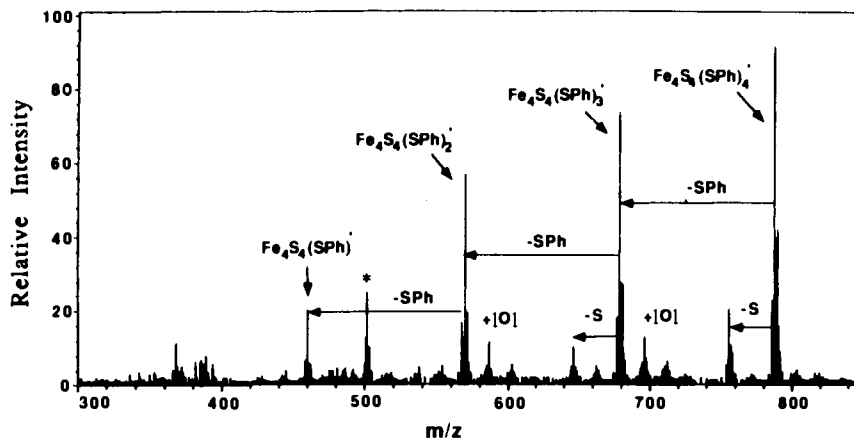


Figure 4. A portion of the negative ion FAB mass spectrum, from m/z 300 to 850, of $(\text{Ph}_4\text{P})_2\text{Fe}_4\text{S}_4(\text{SPh})_4$ using the matrix NPOE. Matrix ions are designated with an asterisk. The major fragment ions and evidence for oxygen incorporation are shown.

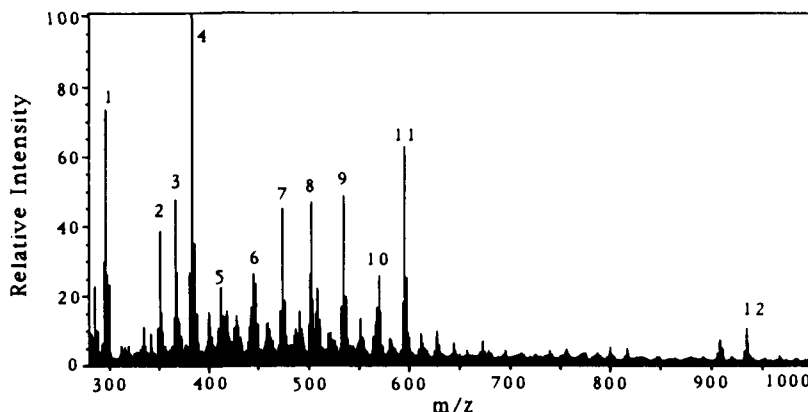


Figure 5. Negative ion FAB mass spectrum of $(\text{Ph}_4\text{P})_2\text{Fe}_4\text{S}_4(\text{SEt})_4$ using the matrix NPOE. Matrix ions are designated with an asterisk. Assignment of peaks: (1) $[\text{Fe}_2\text{S}_2(\text{SEt})_2]^-$; (2) $[\text{Fe}_4\text{S}_4]^-$; (3) $[\text{Fe}_4\text{S}_4\text{O}]^-$; (4) $[\text{Fe}_4\text{S}_5]^-$; (5) $[\text{Fe}_4\text{S}_4(\text{SEt})]^-$; (6) $[\text{Fe}_4\text{S}_5(\text{SEt})]^-$; (7) $[\text{Fe}_4\text{S}_4(\text{SEt})_2]^-$; (8) $[\text{Fe}_4\text{S}_5(\text{SEt})_2]^-$; (9) $[\text{Fe}_4\text{S}_4(\text{SEt})_3]^-$; (10) $[\text{Fe}_4\text{S}_5(\text{SEt})_3]^-$; (11) $[\text{Fe}_4\text{S}_4(\text{SEt})_4]^-$; (12) $[(\text{Ph}_4\text{P})\text{Fe}_4\text{S}_4(\text{SEt})_4]^-$.

negative ion FAB mass spectrometry is superior for the analysis of such compounds. Therefore only negative ion mass spectral results will be presented for the complexes that contain sulfur-based terminal ligands. The features of the negative ion FAB mass spectrum of $(\text{Ph}_4\text{P})_2\text{Fe}_4\text{S}_4(\text{SPh})_4$, Figure 4, obtained using the matrix NPOE, are analogous to those presented for $(\text{Ph}_4\text{P})_2\text{Fe}_4\text{S}_4\text{Br}_4$ and $(\text{Ph}_4\text{P})_2\text{Fe}_4\text{S}_4\text{Cl}_4$. For example, the negative ion spectrum of the molecule $(\text{Ph}_4\text{P})_2\text{Fe}_4\text{S}_4(\text{SPh})_4$ displays clusters of peaks representing the $[\text{M} - \text{Ph}_4\text{P}]^-$ fragment, $[(\text{Ph}_4\text{P})\text{Fe}_4\text{S}_4(\text{SPh})_4]^-$, at m/z 1127, and the intact $[\text{Fe}_4\text{S}_4(\text{SPh})_4]^-$ core, as the -1 ion at m/z 788. Dominant fragment ions include $[\text{Fe}_4\text{S}_3(\text{SPh})_4]^-$ (m/z 756), $[\text{Fe}_4\text{S}_4(\text{SPh})_3]^-$ (m/z 679), $[\text{Fe}_4\text{S}_3(\text{SPh})_3]^-$ (m/z 647), $[\text{Fe}_4\text{S}_4(\text{SPh})_2]^-$ (m/z 570), and $[\text{Fe}_4\text{S}_4(\text{SPh})]^-$ (m/z 460) (Figure 4). The negative ion spectra, for two different counteranions (A^+), are summarized in Table III.

In the negative ion FAB analysis of the $\text{A}_2\text{Fe}_4\text{S}_4\text{X}_4$ compounds, certain ions are always seen, and can be thought of as important indicators for cubane-based analytes. These include $[\text{AFe}_4\text{S}_4\text{X}_4]^-$, $[\text{Fe}_4\text{S}_4\text{X}_4]^-$, $[\text{Fe}_4\text{S}_4\text{X}_3]^-$, $[\text{Fe}_4\text{S}_4\text{X}_2]^-$, $[\text{Fe}_4\text{S}_4\text{X}]^-$, and $[\text{Fe}_2\text{S}_2\text{X}_2]^-$. These are observed when $\text{X} = \text{SPh}$ and SEt as well as when $\text{X} = \text{Br}$ and Cl . However, the two thiolato-containing cubanes also reveal important differences in their mass spectra. More extensive fragmentation is observed when $\text{X} = \text{SEt}$ than when $\text{X} = \text{SPh}$. This can be seen in the negative ion spectrum of $(\text{Ph}_4\text{P})_2\text{Fe}_4\text{S}_4(\text{SEt})_4$, shown in Figure 5. A series of unusual fragment ions deriving from C-S cleavage processes and not found in the spectrum of the SPh analog are $[\text{Fe}_4\text{S}_5(\text{SEt})_3]^-$ (m/z 567), $[\text{Fe}_4\text{S}_5(\text{SEt})_2]^-$ (m/z 506), $[\text{Fe}_4\text{S}_5(\text{SEt})]^-$ (m/z 445), and $[\text{Fe}_4\text{S}_5]^-$ (m/z 384). These observations are consistent with the fact that the SEt ligand contains a relatively weak bond. For RS radicals, the C-S bond of CH_3S is almost 20 kcal/mol weaker than the C-S bond in the PhS radical.²⁵ Thus, alkyl C-S bond cleavage is certainly not surprising in the SEt-containing complexes. Also

Table III. Relative Intensities of Peaks in the Negative Ion FAB Mass Spectra of Complexes $(\text{A})_2\text{Fe}_4\text{S}_4(\text{SR})_4$, $\text{R} = \text{Et}$ and Ph , Using the Matrix NPOE^a

ions observed	relative intensities			
	$(\text{A})_2\text{Fe}_4\text{S}_4(\text{SEt})_4$ for $\text{A} =$		$(\text{A})_2\text{Fe}_4\text{S}_4(\text{SPh})_4$ for $\text{A} =$	
	Ph_4P	Ph_4As	Ph_4P	Bu_4N
$(\text{A})\text{Fe}_4\text{S}_4(\text{SR})_4^-$	12	10	41	14
$\text{Fe}_4\text{S}_4(\text{SR})_4^-$	63	61	100	29
$\text{Fe}_4\text{S}_5(\text{SR})_3^-$	25	25		
$\text{Fe}_4\text{S}_5(\text{SR})_4^-$			20	
$\text{Fe}_4\text{S}_4(\text{SR})_3^-$	48	43	74	33
$\text{Fe}_4\text{S}_5(\text{SR})_2^-$	25	30		
$\text{Fe}_4\text{S}_5(\text{SR})_3^-$			13	
$\text{Fe}_4\text{S}_4(\text{SR})_2^-$	45	25	57	40
$\text{Fe}_4\text{S}_5(\text{SR})_1^-$	25	15		
$\text{Fe}_4\text{S}_4(\text{SR})_1^-$	23	12	20	19
Fe_4S_5^-	100	100		
Fe_4S_4^-	38	32		
$\text{Fe}_2\text{S}_2(\text{SR})_2^-$	74	65	5	100

^a Intensities are relative to 100 for the most abundant ions.

notable in this spectrum are the peaks representing $[\text{Fe}_4\text{S}_4]^-$, m/z 352. This is the only example of an iron/sulfur cubane compound that exhibits an anion which represents the $[\text{Fe}_4\text{S}_4]$ core. The extremely active species $[\text{Fe}_4\text{S}_4]^-$ can further react with desorbed matrix molecules, as described earlier, to produce the $[\text{Fe}_4\text{S}_4(\text{O})]^-$ ion (m/z 368). We note that this is analogous to the $[\text{Fe}_4\text{S}_5]^-$ ion that is observed as a fragment ion. Complete data representing the negative ion FAB analyses of the cubanes containing SR ligands are listed in Table III.

The data presented above for cubanes with sulfur-containing ligands were obtained using NPOE as a matrix. When the matrix

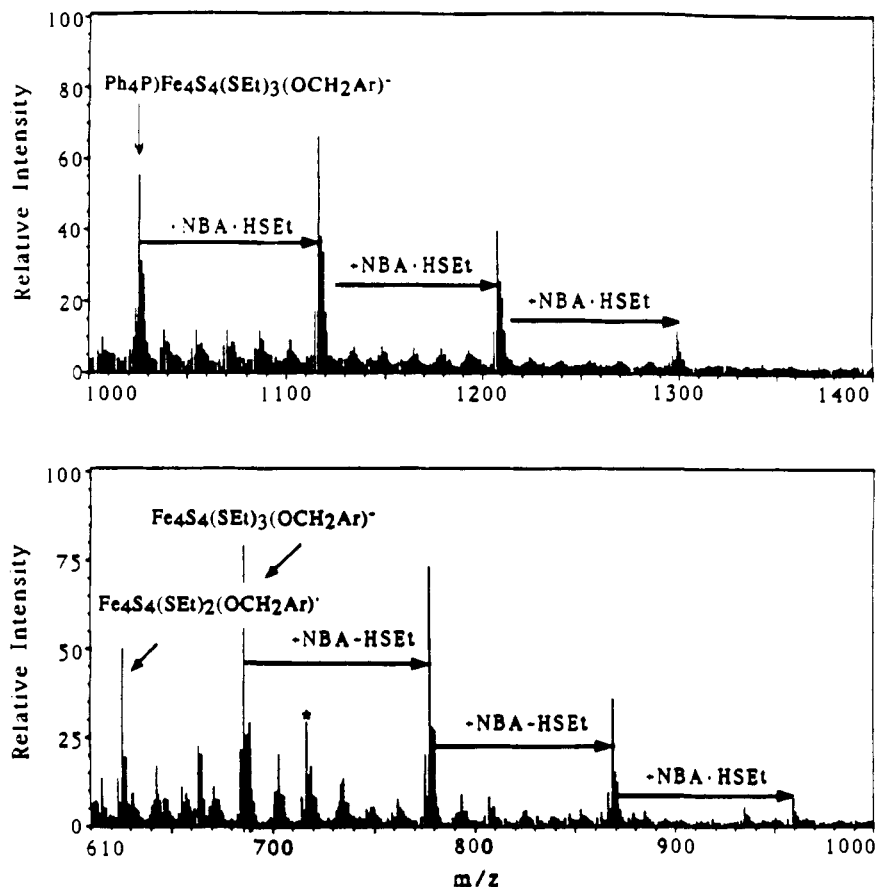
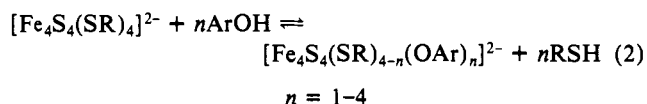
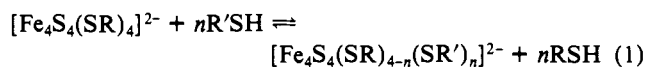


Figure 6. A portion of the negative ion FAB mass spectrum, for m/z 610–1400, of $[(\text{Ph}_4\text{P})_2\text{Fe}_4\text{S}_4(\text{SEt})_4]^-$ using the matrix NBA, showing ions formed in ligand exchange processes involving the matrix. Matrix ions are designated with an asterisk. Ar = PhNO_2 . Intensities for m/z 1000–1400 are boosted by a factor of 4.

is nitrobenzyl alcohol (NBA), the complicated but interesting spectrum shown in Figure 6 is obtained. A rich chemistry occurs between NBA and compounds such as $(\text{Ph}_4\text{P})_2\text{Fe}_4\text{S}_4(\text{SEt})_4$ (M). In the mass range 900–1400, a group of peaks have been assigned as $[\text{M} - (\text{Ph}_4\text{P})]^-$ (m/z 935), $[\text{M} - (\text{Ph}_4\text{P}) + \text{NBA} - \text{HSEt}]^-$ (m/z 1026), $[\text{M} - (\text{Ph}_4\text{P}) + 2(\text{NBA} - \text{HSEt})]^-$ (m/z 1117), $[\text{M} - (\text{Ph}_4\text{P}) + 3(\text{NBA} - \text{HSEt})]^-$ (m/z 1208), and $[\text{M} - (\text{Ph}_4\text{P}) + 4(\text{NBA} - \text{HSEt})]^-$ (m/z 1299). The second group of peaks in the mass range from 590 to 970 correspond to $[\text{M} - 2(\text{Ph}_4\text{P})]^-$ (m/z 596), $[\text{M} - 2(\text{Ph}_4\text{P}) + \text{NBA} - \text{HSEt}]^-$ (m/z 687), $[\text{M} - 2(\text{Ph}_4\text{P}) + 2(\text{NBA} - \text{HSEt})]^-$ (m/z 778), $[\text{M} - 2(\text{Ph}_4\text{P}) + 3(\text{NBA} - \text{HSEt})]^-$ (m/z 869), and $[\text{M} - 2(\text{Ph}_4\text{P}) + 4(\text{NBA} - \text{HSEt})]^-$ (m/z 960). Relative abundances of ion species are listed in Table IV. The results reveal the occurrence of stepwise ligand substitution reactions. The acid-base reaction (eq 1) proceeds to the right when R'SH is a stronger acid than RSH, the conjugate acid of the coordinated thiolate, and this methodology has been well exploited to synthesize $[\text{Fe}_4\text{S}_4]$ complexes with virtually any desired ligands or combination of ligands.^{7,8} Averill and co-workers⁹ have also applied this method to synthesize phenoxide complexes such as $[\text{Fe}_4\text{S}_4(\text{OAr})_4]^{2-}$ (eq 2). Although such ligand substitution



reactions with thiols and phenols have been studied in solution by $^1\text{H-NMR}$,^{7e,9} similar studies involving alcohols were not reported. However, it is intuitively expected that alcohols with acidic OH groups will behave similarly, perhaps with smaller equilibrium constants. Obviously in this work, ligand substitution reactions are occurring, involving the SR ligand on the iron-sulfur complex

Table IV. Relative Intensities of Peaks in the Negative Ion FAB Mass Spectrum of $(\text{Ph}_4\text{P})_2\text{Fe}_4\text{S}_4(\text{SEt})_4$ (Designated as M) Using the Matrix NBA

ions observed	m/z	rel intensity ^a
$[\text{M} - (\text{Ph}_4\text{P}) + 4(\text{NBA} - \text{HSEt})]^-$	1299	2
$[\text{M} - (\text{Ph}_4\text{P}) + 3(\text{NBA} - \text{HSEt})]^-$	1208	6
$[\text{M} - (\text{Ph}_4\text{P}) + 2(\text{NBA} - \text{HSEt})]^-$	1117	11
$[\text{M} - (\text{Ph}_4\text{P}) + (\text{NBA} - \text{HSEt})]^-$	1026	8
$[\text{M} - (\text{Ph}_4\text{P})]^-$	935	4
$[\text{M} - 2(\text{Ph}_4\text{P}) + 4(\text{NBA} - \text{HSEt})]^-$	960	5
$[\text{M} - 2(\text{Ph}_4\text{P}) + 3(\text{NBA} - \text{HSEt})]^-$	869	44
$[\text{M} - 2(\text{Ph}_4\text{P}) + 2(\text{NBA} - \text{HSEt})]^-$	778	88
$[\text{M} - 2(\text{Ph}_4\text{P}) + (\text{NBA} - \text{HSEt})]^-$	687	100
$[\text{M} - 2(\text{Ph}_4\text{P}) + \text{NBA} - 2\text{HSEt}]^-$	626	47
$[\text{M} - 2(\text{Ph}_4\text{P})]^-$	596	63

^a Intensities are relative to 100 for the most abundant analyte ions. Nominal mass is used for the m/z value.

and the matrix molecules (alcohols). There are three possible explanations for this occurrence. First, it could be a simple analyte/matrix reaction that occurs when the two are mixed. Second, it could be chemistry induced by the fast atom beam (again, condensed phase chemistry). Third, it could occur for the gas-phase ions, with desorbed matrix molecules, and not be representative of solution chemistry at all. Since these peaks are so dominant, such extensive conversion of reactants to products would be unlikely if the chemistry occurred in the gas phase. On the other hand, we have used $^1\text{H-NMR}$ to study the reaction between $[\text{Fe}_4\text{S}_4(\text{SEt})_4]^{2-}$ and NBA in $\text{DMSO}-d_6$. Ligand substitution chemistry does occur, to form $[\text{Fe}_4\text{S}_4(\text{SEt})_{4-n}(\text{OCH}_2\text{Ar})_n]^{2-}$, although the reaction is exceedingly slow, showing approximately 15% of the reactant being converted into products after 72 h. Thus, this may well be an example of fast atom bombardment induced chemistry, in which the particle bombardment of the matrix facilitates the rate of the ligand exchange reactions.

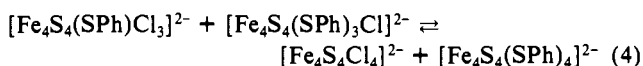
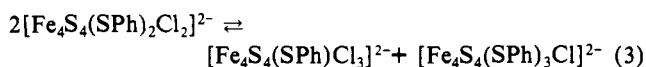
Table V. Relative Intensities of Peaks in the Negative Ion FAB Mass Spectrum of Complex $(\text{Ph}_4\text{P})_2\text{Fe}_4\text{S}_4(\text{SPh})_2\text{Cl}_2$ in DMF/NPOE^a

fragment ions	<i>m/z</i>	rel intensity
$[(\text{Ph}_4\text{P})\text{Fe}_4\text{S}_4(\text{SPh})_3\text{Cl}]^-$	1053	7
$[(\text{Ph}_4\text{P})\text{Fe}_4\text{S}_4(\text{SPh})_2\text{Cl}_2]^-$	979	15
$[(\text{Ph}_4\text{P})\text{Fe}_4\text{S}_4(\text{SPh})\text{Cl}_3]^-$	905	22
$[(\text{Ph}_4\text{P})\text{Fe}_4\text{S}_4\text{Cl}_4]^-$	831	17
$[\text{Fe}_4\text{S}_4(\text{SPh})_3\text{Cl}]^-$	714	20
$[\text{Fe}_4\text{S}_4(\text{SPh})_2\text{Cl}_2]^-$	640	52
$[\text{Fe}_4\text{S}_4(\text{SPh})\text{Cl}_3]^-$	608	18
$[\text{Fe}_4\text{S}_4(\text{SPh})_2\text{Cl}_2]^-$	605	22
$[\text{Fe}_4\text{S}_4(\text{SPh})\text{Cl}_3]^-$	566	63
$[\text{Fe}_4\text{S}_4(\text{SPh})\text{Cl}_3]^-$	534	30
$[\text{Fe}_4\text{S}_4(\text{SPh})\text{Cl}_2]^-$	531	62
$[\text{Fe}_4\text{S}_4(\text{SPh})\text{Cl}_2]^-$	499	25
$[\text{Fe}_4\text{S}_4(\text{SPh})\text{Cl}]^-$	496	45
$[\text{Fe}_4\text{S}_4\text{Cl}_4]^-$	492	47
$[\text{Fe}_4\text{S}_4\text{Cl}_4]^-$	460	35
$[\text{Fe}_4\text{S}_4\text{Cl}_3]^-$	457	85
$[\text{Fe}_4\text{S}_4\text{Cl}_3]^-$	425	56
$[\text{Fe}_4\text{S}_4\text{Cl}_2]^-$	422	100
$[\text{Fe}_4\text{S}_4\text{Cl}_2]^-$	390	33
$[\text{Fe}_4\text{S}_4\text{Cl}]^-$	387	68
$[\text{Fe}_3\text{S}_3\text{Cl}_3]^-$	337	30
$[\text{Fe}_3\text{S}_3\text{Cl}_2]^-$	334	72

^a Intensities are relative to 100 for the most abundant analyte ions. Nominal mass is used for the *m/z* value. Peaks with *m/z* values less than 300 are not listed in this table.

C. The FAB-MS Analysis of Mixed-Ligand Cubane Clusters.

The utility of FAB-MS to analyze the mixed ligand cubane $(\text{Ph}_4\text{P})_2\text{Fe}_4\text{S}_4(\text{SPh})_2\text{Cl}_2$ was evaluated. A simple spectrum representative of this analyte was not expected, since NMR studies⁷ have shown that, in solution, this complex disproportionates and exists in equilibrium with other mixed ligand cubane clusters represented by eqs 3 and 4. The negative ion FAB-MS analysis



using the matrix NPOE confirms the existence of these disproportionation species in solution. The ions observed are listed in Table V. In the high mass range between 800 and 1100, there are four major sets of peaks corresponding to $[(\text{Ph}_4\text{P})\text{Fe}_4\text{S}_4\text{Cl}_4]^-$ (*m/z* 831), $[(\text{Ph}_4\text{P})\text{Fe}_4\text{S}_4(\text{SPh})\text{Cl}_3]^-$ (*m/z* 905), $[(\text{Ph}_4\text{P})\text{Fe}_4\text{S}_4(\text{SPh})_2\text{Cl}_2]^-$ (*m/z* 979), and $[(\text{Ph}_4\text{P})\text{Fe}_4\text{S}_4(\text{SPh})_3\text{Cl}]^-$ (*m/z* 1053). A second group of peaks in the middle-mass range are assigned as $[\text{Fe}_4\text{S}_4\text{Cl}_4]^-/[\text{Fe}_4\text{S}_4(\text{SPh})\text{Cl}_3]^-/[\text{Fe}_4\text{S}_4(\text{SPh})_2\text{Cl}_2]^-$ (overlapping cluster peaks with nominal *m/z* values of 492, 496, and 499, respectively), $[\text{Fe}_4\text{S}_4(\text{SPh})\text{Cl}_3]^-/[\text{Fe}_4\text{S}_4(\text{SPh})_2\text{Cl}_2]^-$ (overlapping cluster peaks with nominal *m/z* values of 531 and 534, respectively), $[\text{Fe}_4\text{S}_4(\text{SPh})\text{Cl}_3]^-$ (*m/z* 566), $[\text{Fe}_4\text{S}_4(\text{SPh})_2\text{Cl}_2]^-/[\text{Fe}_4\text{S}_4(\text{SPh})\text{Cl}_3]^-$ (overlapping cluster peaks with nominal *m/z* values of 605 and 608, respectively), $[\text{Fe}_4\text{S}_4(\text{SPh})_2\text{Cl}_2]^-$ (*m/z* 640), and $[\text{Fe}_4\text{S}_4(\text{SPh})_3\text{Cl}]^-$ (*m/z* 714). The group of peaks in the low mass region show fragment ions related to the core decomposition of $[\text{Fe}_4\text{S}_4\text{Cl}_4]^-$ as described above. A series of oxidized fragment ions, appearing 16 u and/or 32 u above the major fragments, were also observed as described above.

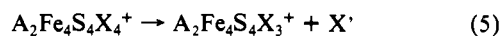
Depending on the extent of disproportionation shown in eqs 3 and 4, we might expect to see mass spectral features indicative of $(\text{Ph}_4\text{P})\text{Fe}_4\text{S}_4(\text{SPh})_4$. Representative ions of this species are not seen in the spectrum of $(\text{Ph}_4\text{P})_2\text{Fe}_4\text{S}_4(\text{SPh})_2\text{Cl}_2$. Most of the fragments can be explained by the loss and addition of SPh or Cl ligands from the mixed ligand complex. At present, three sets of peaks representing $[\text{Fe}_4\text{S}_4(\text{SPh})\text{Cl}_3]^-$, $[\text{Fe}_4\text{S}_4(\text{SPh})_2\text{Cl}_2]^-$, and $[\text{Fe}_4\text{S}_4(\text{SPh})_3\text{Cl}]^-$ have been identified, but no evidence was obtained for the existence of $[(\text{Ph}_4\text{P})\text{Fe}_4\text{S}_4(\text{SPh})_4]^-$ and/or $[\text{Fe}_4\text{S}_4(\text{SPh})_4]^-$. This may be due to further equilibria established between $[\text{Fe}_4\text{S}_4(\text{SPh})_4]^{2-}$ and $[\text{Fe}_4\text{S}_4(\text{SPh})_{4-n}\text{Cl}_n]^{2-}$ species. This is expected in view of the known lability of the $[\text{Fe}_4\text{S}_4\text{X}_4]^{2-}$

complexes.^{7c,27} Our FAB mass spectral results are in excellent agreement with the aforementioned solution equilibria.

2. Proposed Fragmentation Mechanisms: Correlations between Negative Ion FAB-MS Data and Known Iron-Sulfur Cluster Chemistry in Condensed Phases. Before evaluating the types of ions observed in these experiments, a comment should be made on what might be expected in a mass spectral study of ions derived from salts containing the Fe_4S_4 core in which the iron atoms are in +2 and +3 formal oxidation states, as $(\text{Fe}^{2+})_2(\text{Fe}^{3+})_2(\text{S}^{2-})_4$. When electron impact ionization is used to ionize a compound such as $\text{Fe}(\text{CO})_5$, a dominant ion in the resulting mass spectrum is Fe^+ , which represents an oxidation state not typically considered in condensed phases. Thus, one might expect to generate fragments of the Fe_4S_4 core in which unusual oxidation states of the metal are present. On the other hand, it is a general "rule of thumb" in the mass spectrometry of inorganic and organometallic compounds²⁸ that the dominant ions are formed with a minimal perturbation to the formal oxidation state of the metal in the compound undergoing ionization. In the iron pentacarbonyl case, the iron atom is formally taken from an oxidation state of 0 in the neutral compound to +1 as the univalent cation (and in all fragment ions such as $\text{Fe}(\text{CO})_3^+$). In contrast, the Ti^+ peak in the mass spectrum of TiCl_4 is a very minor peak, because its formation would require the conversion of Ti^{4+} to Ti^+ . In this case, ions such as TiCl_3^+ dominate, in which no net change in the oxidation state of the metal occurs. Thus, we might expect, based on the oxidation states of iron atoms in the Fe_4S_4 core, that fragment ions will be formed in which the metal atoms are in their readily accessible +2 and +3 oxidation states.

Ionic complexes such as the $(\text{A})_2\text{Fe}_4\text{S}_4\text{X}_4$ salts that are the subject of this study, once dissolved in solution, produce a variety of ionic species such as $(\text{A})^+$, $(\text{A})^+[\text{Fe}_4\text{S}_4\text{X}_4]^{2-}$, and $[\text{Fe}_4\text{S}_4\text{X}_4]^{2-}$, as suggested in Scheme I. When the solution is subjected to fast atom bombardment, desorption of neutral species and ionic complexes from the analyte/matrix target leads to a variety of gas-phase species. Presumably, the neutral, intact molecule desorbs to some extent. Also, the ionic components desorb as ions ("preionized species", as they are commonly called in FAB), and from these the ions observed in the FAB spectra are derived.

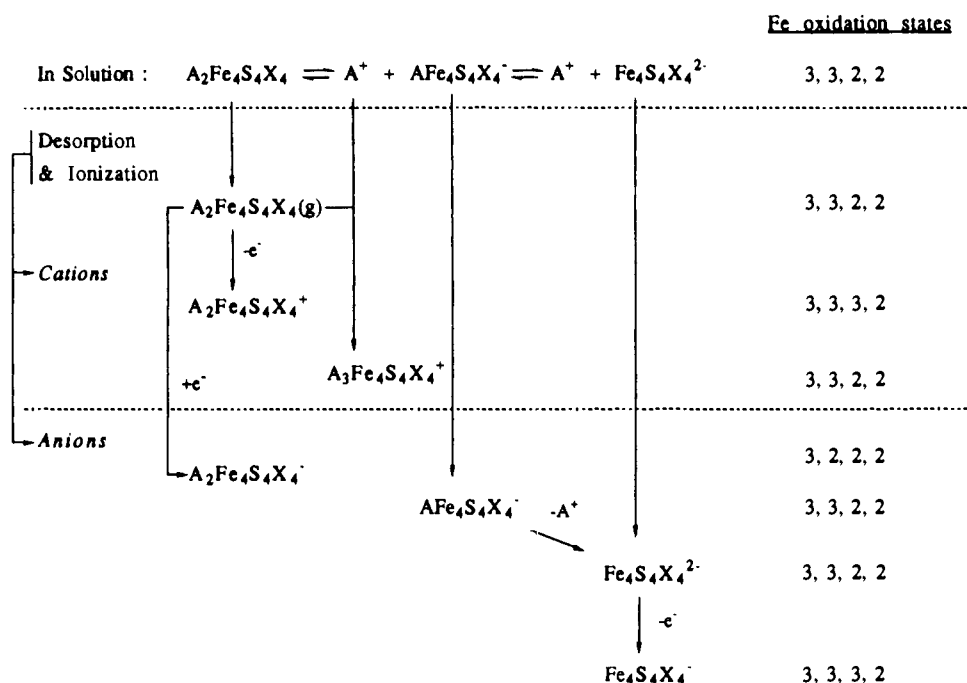
Following desorption, the intact neutral molecule $(\text{A})_2\text{Fe}_4\text{S}_4\text{X}_4$ may be converted into the molecular ion, $[(\text{A})_2\text{Fe}_4\text{S}_4\text{X}_4]^+$, either via a gas-phase charge-transfer reaction or by a subsequent interaction of the desorbed molecule with a fast atom. The counterion, A^+ , apparently forms adducts with gas-phase species formed in the FAB process, yielding both A^+ -matrix complexes and adducts with the desorbed neutral analyte, $[(\text{A})_2\text{Fe}_4\text{S}_4\text{X}_4]^+$. Thus, $[(\text{A})_2\text{Fe}_4\text{S}_4\text{X}_4]^+$ are the two possible "primary" cations formed, from which fragment ions may be generated. The major fragment ion is $[(\text{A})_2\text{Fe}_4\text{S}_4\text{X}_3]^+$, which we propose is formed by the loss of an X radical from the molecular cation. Consider the reaction of the loss of an X ligand, not as an anion, but as a radical. When X is lost, the formal oxidation state of one of the iron atoms must change (reduction). We propose two ways to consider this simple process (which will become very powerful when anionic fragments are considered). For the unimolecular dissociation reaction (eq 5), one can keep track of the oxidation states of the



(27) Unfortunately, thermochemical information on the $\text{C}_2\text{H}_5\text{S}$ radical is not available. Heats of formation of gas-phase CH_3S , CH_3 , and S suggest a C-S bond strength of 72.4 kcal/mol, which should be typical of alkyl-S bond strengths. In contrast, available data suggest a C-S bond strength of 90.2 kcal/mol in PhS. If the C-S bond strengths in $\text{C}_2\text{H}_5\text{SH}$ and $\text{C}_6\text{H}_5\text{SH}$ are compared, the alkyl thiol has a bond strength 13 kcal/mol less than the aromatic compound. Complete thermochemical information on the anions is not available; however, if one considers the species that are isolectronic with $\text{C}_2\text{H}_5\text{S}^-$ and $\text{C}_6\text{H}_5\text{S}^-$, which are $\text{C}_2\text{H}_5\text{Cl}$ and $\text{C}_6\text{H}_5\text{Cl}$, again the C-X bond is lower by greater than 10 kcal/mol for the alkyl group. Thus, it is safe to assume that alkyl-S bonds are weaker than phenyl-S bonds. All thermochemical data were taken from: Lias, S. G.; Bartmess, J. E.; Liebman, J. F.; Holmes, J. L.; Levin, R. D.; Mallard, W. G. *J. Phys. Chem. Ref. Data* **1988**, *17*, Suppl. No. 1.

(28) Charalambous, J. *Mass Spectrometry of Metal Compounds*; Butterworth: Boston, 1975.

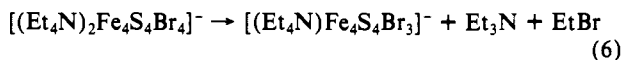
Scheme I



iron atoms, or of the $[Fe_4S_4]$ core. The formal charges on the four metal atoms change in this dissociation reaction from $\{+3, +3, +3, +2\}$ to $\{+3, +3, +2, +2\}$. If the $[Fe_4S_4]$ core is considered, it changes from $[Fe_4S_4]^{3+}$ to $[Fe_4S_4]^{2+}$ (i.e., a net reduction of the core) when a ligand is lost as a radical. Apparently no fragments evolve from the adduct ion $[(A)_3Fe_4S_4X_4]^+$, in which the iron atoms are also in the oxidation states $\{+3, +3, +2, +2\}$.

Returning to Scheme I, the early steps in the chemistry that leads to the desorption/ionization of *anionic* species can be described, by considering the species that can be desorbed from the analyte/matrix solution. Once desorbed, the intact neutral molecule can capture an electron to form the molecular anion, $[(A)_2Fe_4S_4X_4]^-$. The "preformed ion", $[(A)Fe_4S_4X_4]^-$, can be desorbed directly from the matrix. Presumably, the $[Fe_4S_4X_4]^{2-}$ dianion can be desorbed directly, to some extent, although the spectra suggest that, if this occurs, it is completely converted into the univalent anion, $[Fe_4S_4X_4]^-$. Note that these "primary" cations and anions shown in Scheme I, from which all fragment ions will be formed, *all* contain iron atoms that only involve combinations of the +2 and +3 formal oxidation states. Thus, while it is certainly possible to generate complexes of iron in mass spectrometry that contain Fe^+ , none are present in these ions listed in Scheme I.

Scheme II presents proposed unimolecular fragmentation pathways to explain the evolution of the rich collection of fragment *anions* formed by fast atom bombardment. The pathways proposed here are based on a few simple assumptions. First, for an ion with a charge of -1 to form a fragment ion with a charge of -1, either a radical or an uncharged even-electron fragment must be lost. Obvious candidates for neutral species lost include fragments such as X and FeS. One may consider loss of the neutral $[FeSX]$, but not $[Fe]$ alone, because of the bonding environment in the starting material. That is, we would not expect a fragment ion with 2 or 3 iron atoms but all four X ligands still present. Next, the loss of neutral "A" was not considered—that is, while one may expect to lose a chlorine radical, one would not lose a tetraalkylammonium radical. Third, the loss of "AX" was considered as an allowable fragmentation. An example of "AX" elimination is shown in eq 6. If, for example, A^+ is Et_4N^+ and the ion contains $X = Br$, "AX" loss is equivalent to the loss of $\{Et_3N$ and $EtBr\}$, as shown in (6). Scheme II lists the 4-, 3-, and

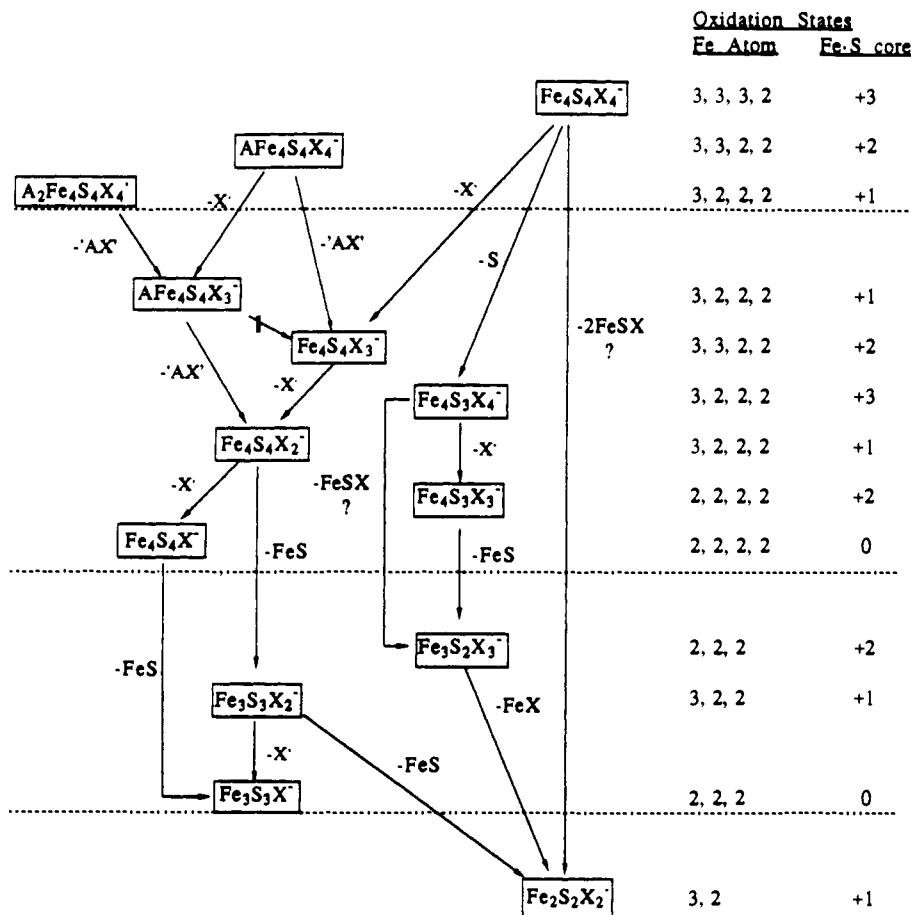


2-Fe-containing fragment ions that are observed, with various numbers of sulfur atoms and X ligands incorporated. The column on the right side of Scheme II lists the formal oxidation states of the iron atoms associated with each chemical species. It clearly shows that all of the unimolecular dissociation chemistry occurs without having to invoke the formation of exotic valence states of any of the iron atoms within the remaining core. This becomes very important in understanding and interpreting the mass spectra of such compounds. It suggests that, in the negative ion spectra of iron sulphur cubanes, an anion representative of the cubane core $[Fe_4S_4]^-$ would not be expected, since this would force one of the iron atoms to be reduced from +2 to +1. In fact, the fragment ion, $[Fe_4S_4]^-$, is only detected from ionization of $[Fe_4S_4(SET)_4]^{2-}$. Essentially all of the ions observed are those that can exist in the context of the one restriction—maintaining the iron atoms as either +2 or +3 metals.

The observation of $[Fe_4S_4]^-$, in one case only, deserves comment. Whatever its structure, the four iron atoms must be in the oxidation states $\{+2, +2, +2, +1\}$. As seen in Table III, this anion is only formed from compounds that also form the $[Fe_4S_5]^-$ anion. The two may be chemically linked, with $[Fe_4S_4]^-$ being a fragment of the more abundant $[Fe_4S_5]^-$ species. We note that this one violation of the oxidation state restriction, which seems to hold for all other fragment ions, involves a complete cubane core, as opposed to some cubane fragment. Of all of the $[Fe_mS_n]$ species encountered in this work, it would surely be the intact cubane that could most effectively delocalize an extra electron. Thus it is not surprising that the only exception to the rule occurs not for a small fragment ion but for a larger species containing four iron atoms, in which the cubic geometry is presumably intact.

Further insights into the fragmentation mechanisms, which provide a very interesting link between the ions listed in Scheme II, can be seen by considering the overall oxidation state of the $[Fe_mS_n]$ cores of the various ions. For all of the fragmentations suggested, if the oxidation state of the iron/sulfur core is considered, **only reductive eliminations, or fragmentations in which there is no change in the oxidative state, are observed.** The extent to which a "primary ion" leads to fragment ions is clearly linked to its $[Fe_mS_n]$ core oxidation state. The ion that leads to most of the fragment anions observed is $[Fe_4S_4X_4]^-$, which contains a $[Fe_4S_4]^{3+}$ core. Clearly, it leads to fragment ions with $[Fe_mS_n]$ core oxidation states of +3, +2, and +1. When it fragments to form an ion with an Fe_mS_n core that is in a +3 or +2 state, that fragment dissociates further. The most dramatic example is shown

Scheme II



in the pathway in Scheme II that leads from $[\text{Fe}_4\text{S}_4\text{X}_4]^-$ to $[\text{Fe}_3\text{S}_3\text{X}]^-$, in which the $[\text{Fe}_m\text{S}_n]$ cores of the species involved smoothly change their oxidation state from +3 to +2 to +1 to 0! Thus, we propose here that, in the FAB analyses of iron-sulfur cluster compounds, the primary ions formed by FAB fragment through reductive chemistry in which all of the metal atoms retain +2 and +3 oxidation states, and the $[\text{Fe}_m\text{S}_n]$ core oxidation states do not increase as the unimolecular dissociations occur. Both one- and two-electron reductions are proposed in Scheme II.

It should be clearly stated that while the mechanistic aspects of Scheme II are conjecture, the fragment ions listed and the oxidation state observations are not. Regardless of the actual fragmentation mechanisms, which remain to be established, the fragment ions listed are formed through processes that preserve +2 and +3 oxidation states for the iron atoms involved.

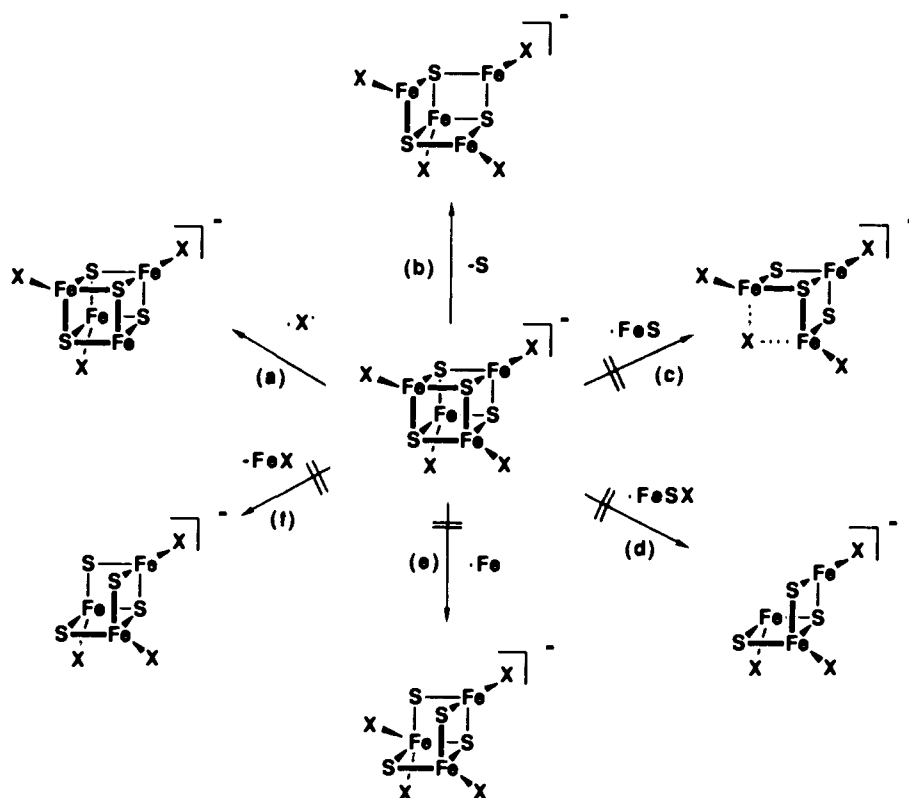
These insights make it straightforward to interpret these mass spectra and will be important guidelines with which spectra of related compounds can be correlated with structure. For each ion that is a primary ion of FAB, we can *predict* which fragment ions can be formed and which cannot. An example is shown in Scheme III, beginning with ionic species $[\text{Fe}_4\text{S}_4\text{X}_4]^-$. One might expect that the ion *could* lose as possible neutral fragments X, S, FeS, FeX, FeSX, or Fe. We consider each of these possibilities in Scheme III. Pathway a: The conversion of $[\text{Fe}_4\text{S}_4\text{X}_4]^-$ to $[\text{Fe}_4\text{S}_4\text{X}_3]^-$ suggests the dissociation of a labile ligand X as a radical. It forms a fragment ion which only incorporates Fe(II) and Fe(III), thus should be expected and is observed. Pathway b: The same is true for the degradation to $[\text{Fe}_4\text{S}_3\text{X}_4]^-$ by the loss of S, which produces a {+3, +2, +2, +2} iron core by a two-electron reduction. Pathway c: The destruction of the cubane core by the loss of FeS also leads to a fragment ion in which no Fe atoms need to be in states other than +2 or +3; however, it is not observed. Presumably, the halogens are bonded to the iron atoms, and an iron cannot be lost with the ionic fragment retaining four halogens. Pathway d: The fragment from the loss of a relatively large FeSX fragment is reasonable, yet it is not observed (i.e. no $[\text{Fe}_3\text{S}_3\text{X}_3]^-$

is detected). The stepwise loss of X and then FeS is a more favorable pathway as shown in Scheme II for other ions. Pathway e: Fe atom ejection from the cubane core would be unexpected for two reasons. As mentioned above, an iron cannot retain four halogens with only three Fe atoms in the core. Also, if Fe(0) were lost, the oxidation state of the remaining metals must change to {+4, +4, +3}, which clearly does not occur in these systems, consistent with the fact that the product $[\text{Fe}_3\text{S}_4\text{X}_4]^-$ is never observed. Pathway f: The loss of the neutral FeX would also be unexpected, since the oxidation state of one of the remaining Fe atoms must be changed to Fe^{4+} .

The correlation of gas-phase $[\text{Fe}_m\text{S}_n]$ anionic species, generated from the cubane cluster by FAB with known chemistry of iron-sulfur complexes is intriguing. In the condensed phase (i.e. solution), complexes have been made in which the $[\text{Fe}_4\text{S}_4]$ core is in an oxidation state of +1, +2, or +3.^{7,29} All three oxidation states are observed in the negative ion spectra, Scheme II. However, in the gas phase, the unusual 0 oxidation state of the $[\text{Fe}_4\text{S}_4]$ core also exists. The $[\text{Fe}_2\text{S}_2]$ core is known in solution with +2 and +1 oxidation states; the +1 state is observed in the gas phase. Thus, the oxidation states observed in solution to date provide some useful limits as to what to expect in the gas phase. The gas-phase data may also suggest species that *could* exist in condensed phases and could be pursued synthetically.

With the insights gained from analysis of the negative ion FAB spectra, correlating possible fragment ions with limitations in available oxidation states, it becomes obvious why negative ion FAB is the mass spectral technique of choice, when both molecular weight and structural information are desired. This also explains why the positive ion spectra are so simple. In Scheme II, there are three species cited through which fragment ions may be formed, the largest fraction of the fragments originating from $[\text{Fe}_4\text{S}_4\text{X}_4]^-$, where the four iron atoms are in the states {+3, +3,

Scheme III



+3, +2}. Why does the corresponding cation not lead to a variety of fragment cations? In fact, the corresponding cation is *not* formed by FAB. To convert this anion to a cation would require the removal of two electrons, which would result in the four iron atoms having oxidation states of {+4, +3, +3, +3}. This is an intriguing possibility; most of the fragment ions listed in Scheme II could exist as cations without violating the oxidation state rule, but their precursor cannot. Thus, the limitations on oxidation states of the iron atoms give fewer choices for cationic species. Obviously, there are "oxidation state bottlenecks" that would be expected for the unimolecular chemistry of cations formed by FAB; a rich cation chemistry is not expected, which would parallel the unimolecular fragmentation anion chemistry.

Conclusions

We have reported herein the utility of FAB-MS for the characterization of iron/sulfur cubane-containing compounds and have discussed aspects of the fragmentation mechanisms that will assist in the mass spectral interpretation of related compounds. Both 3-nitrobenzoyl alcohol (NBA) and 2-nitrophenyl octyl ether (NPOE) are suitable matrices for the FAB-MS studies of these series of complexes. It should be emphasized that, when such compounds are being characterized, it is vital that the experimentally observed and theoretically calculated isotopic patterns be compared, to assist in the correct identification of the ions formed.

Fast atom bombardment of a matrix containing iron/sulfur cubane clusters has been evaluated here, as a chemical system which generates a variety of smaller clusters in a variety of oxidation states, through unimolecular fragmentation processes. The restrictions on oxidation states that seem to dominate the frag-

mentation pathways yield interesting parallels with known clusters in the condensed phase.

In addition, we have successfully introduced FAB-MS analysis as a new methodology to characterize intermediates of ligand substitution reactions between analyte and matrix such as $[\text{Fe}_4\text{S}_4(\text{SEt})_4]^{2-}$ and 3-nitrobenzyl alcohol, as well as to confirm the existence of disproportionation species in solution (i.e., $(\text{Ph}_4\text{P})_2\text{Fe}_4\text{S}_4(\text{SPh})_2\text{Cl}_2$ in DMF). Furthermore, both NBA and NPOE participate in an unusual gas-phase oxygen atom transfer reaction with the iron-sulfur complexes.

It will be interesting to compare the results presented here with FAB-based analysis of small redox systems that contain an iron/sulfur cubane linkage. It will be intriguing to see how the cubane core fragments when attached to a peptide relative to thiolate, since this may give insight on how peptides regulate the redox properties of Fe/S clusters. Furthermore, it should be noted that, using mass spectrometry, ion-molecule reactions of *any* of the anions discussed in this work could be studied and used to determine properties of anions in the gas phase such as electron affinities and reactivity. Thus, FAB-MS offers not only a facile method for analysis but also an opportunity for the generation of unusual chemical species and the characterization of very rich gas-phase chemistry.

Acknowledgment. This work was supported by NIH Grants GM36520 (C.K.C.) and NIH-BRSG RR07049 (M.G.K.) and NSF Grant CHE-8958451 (M.G.K.). Mass spectral data were obtained at the Michigan State University/National Institutes of Health Mass Spectrometry Facility which is supported, in part, by a grant (RR-00480) from the Biotechnology Resources Branch, Division Research Resources, National Institutes of Health.